

Hierarchy in Mid-Rapidity Fragmentation: Mass, Isospin, Velocity Correlations

V. Baran^{1,2,*}, M. Colonna³, M. Di Toro^{3,4}, R. Zus¹

¹ *Physics Faculty, University of Bucharest, Romania*

² *NIPNE-HH, Bucharest-Magurele, Romania*

³ *Laboratori Nazionali del Sud INFN,
I-95123 Catania, Italy*

⁴ *Physics and Astronomy Dept., University of Catania*

* *email: baran@ifin.nipne.ro*

We present new features of the transition from nuclear multifragmentation to neck fragmentation in semi-central heavy-ion collisions at Fermi energies as obtained within a microscopic transport model, Stochastic Mean Field (SMF). We show that along this transition specific hierarchy phenomena of some kinematic observables associated with the intermediate mass fragments develop. Their correlations with the dynamics of isospin degree of freedom, predicted by our calculations, open new possibilities to learn about the density dependence of nuclear symmetry energy below saturation, as well as about the fragmentation mechanisms. Detailed results are presented for mass symmetric $Sn + Sn$ reactions with different isospin content at $50A$ MeV.

PACS numbers: 25.70.Pq, 25.70.Mn, 21.65.Ef, 24.10.Cn

Keywords: Nuclear fragmentation, Symmetry energy, Reaction mechanisms

I. INTRODUCTION

Nucleus-nucleus collisions provide a unique tool to explore the properties of finite interacting fermionic systems in a broad range of densities and temperatures. At energies between 10 and $100A$ MeV, usually referred to as 'Fermi energies', the mean-field and collisional effects are quite balanced leading to a very intricate dynamics, sensitive to impact parameter and beam energy. Entrance channel effects, as well as phenomena well explained in terms of statistical equilibrium, can co-exist. Moreover, as a consequence of the two-component character of nuclear matter, additionally features due to isospin manifest. Indeed, the symmetry energy term in the equation of state (EOS) was one of the main subjects of interest during the last decade [1–3].

The fragmentation process is an ubiquitous phenomenon observed at Fermi energies. However, the underlying reaction mechanisms can be rather different and a detailed study can provide independent information on the nuclear EOS out of saturation. The aim of this paper is to suggest new fragment mass-velocity-isospin correlations particularly sensitive to the various mechanisms, as well as to the in-medium nuclear interaction.

For central collisions, the nuclear multifragmentation can be associated with a liquid-gas phase transition in a composite system [4]. While the final state configurations are well described within statistical equilibrium models [5], but also within hybrid models coupling a dynamical formation and evolution of primary fragments with a secondary decay stage [6], the kinetics of this phase transition can be related to spinodal decomposition in two-component nuclear matter [4, 7, 8] accompanied by the isospin distillation. Increasing the impact parameter, the neck fragmentation, with a peculiar intermediate mass fragments (IMF, $3 \leq Z \leq 20$) distribution and an entrance channel memory, was observed experimen-

tally [9–12] and predicted by various transport models [13],[14]. In this case the low-density neck region triggers an isospin migration from the higher density regions corresponding to projectile-like fragment, PLF, and target-like fragment, TLF. Therefore, the isospin content of the IMF's is expected to reflect the isospin enrichment of mid-velocity region. For even more peripheral collisions, an essentially binary reaction in exit channel can be accompanied by a dynamically induced fission of the participants [15, 16] and for N/Z asymmetric entrance channel combinations isospin diffusion takes place [17–19].

Consequently, the isospin degree of freedom can be seen as a precious tracer providing additional information about the physical processes taking place during the evolution of the colliding systems. Moreover, from a comparison between the experimental data and the theoretical model predictions, isospin dynamics allows to investigate the density and/or temperature dependence of the symmetry energy. More exclusive analysis from the new experimental facilities certainly will impose severe restrictions on various models and parametrization concerning this quantity.

Following these arguments, the purpose of this article is to inquire on the dynamics of the fragmentation process from semi-central to semi-peripheral collisions. We explore the kinematic properties of the fragments produced at the transition from multifragmentation to neck fragmentation. A hierarchy in the transverse velocity of IMF's is clearly evidenced. Moreover, new interesting correlations between kinematic features of the fragments and isospin dynamics, which can provide clues in searching for the most sensitive observables to the symmetry energy, are noted. We mention that for central collisions a radial expanding multifragmenting source develop. In this case a correlation between the N/Z of the fragments and their kinetic energy, sensitive to the density behavior of the symmetry energy, was recently evidenced in

a transport model [20]. The average value of this ratio decreases with the kinetic energy per nucleon and it is asy-EOS dependent.

An experimental study of internal correlations for the fragmentation of quasi-projectiles was performed by Colin et al. [21], within the INDRA collaboration. For certain classes of events a hierarchy of mass fragments along the beam axis was interpreted in terms of the breakup of the very elongated structure emerging from the interaction of the two colliding nuclei. More recently, McIntosh and al. examined the fragment emission from $Xe + Sn$ peripheral and mid-peripheral dissipative collisions [22]. A significant enhancement of backward fragments yield relative to the forward component as well as an alignment with the direction of projectile-like residue velocity were evidenced.

In section II we briefly review the transport approach and specify the reactions which are studied. Section III is focused on the properties of the observed fragmentation mechanisms. Isospin effects are analyzed in section IV in connection with the kinematic features of the fragments. Finally, in section V the conclusions and some suggestions for experiments are presented.

II. THE TRANSPORT APPROACH

To achieve the goal of this work we employ a semi-classical microscopic transport model, Stochastic Mean Field (SMF), based on Boltzmann-Nordheim-Vlasov (BNV) equation [23]. Our choice is motivated by the requirement to have a well implemented nuclear mean-field dynamics together with the effects of fluctuations induced by two-body scattering. Experimental indications at energies between 20 AMeV and 100 AMeV, including the behavior of collective flows, suggest that mean-field plays an essential role in shaping the evolution of the system. Within the Stochastic Mean-Field model, the time evolution of the one-body distribution function $f(\mathbf{r}, \mathbf{p}, t)$ is described by a Boltzmann-Langevin equation [24]:

$$\frac{\partial f}{\partial t} + \frac{\mathbf{p}}{m} \frac{\partial f}{\partial \mathbf{r}} - \frac{\partial U}{\partial \mathbf{r}} \frac{\partial f}{\partial \mathbf{p}} = I_{coll}[f] + \delta I[f], \quad (1)$$

where the fluctuating term $\delta I[f]$ is implemented through stochastic spatial density fluctuations [25]. The collision integral $I_{coll}[f]$ for fermionic systems takes into account the energy, the angular and isospin dependence of free nucleon-nucleon cross sections.

The symmetry energy effects were studied by employing two different density parametrizations [26] of the mean field:

$$U_q = A \frac{\rho}{\rho_0} + B \left(\frac{\rho}{\rho_0} \right)^{\alpha+1} + C(\rho) \frac{\rho_n - \rho_p}{\rho_0} \tau_q + \frac{1}{2} \frac{\partial C}{\partial \rho} \frac{(\rho_n - \rho_p)^2}{\rho_0}, \quad (2)$$

where $q = n, p$ and $\tau_n = 1, \tau_p = -1$. For asysoft EOS,

$\frac{C(\rho)}{\rho_0} = 482 - 1638\rho$, the symmetry energy $E_{sym}^{pot} = \frac{1}{2} C(\rho) \frac{\rho}{\rho_0}$ has a weak density dependence close to the saturation, being almost flat around ρ_0 . For asysuperstiff case, $\frac{C(\rho)}{\rho_0} = \frac{32}{\rho_0} \frac{2\rho}{\rho + \rho_0}$, the symmetry energy is quickly decreasing for densities below normal density. The coefficients A, B and the exponent α , characterizing the isoscalar part of the mean-field, are fixed requiring that the saturation properties of symmetric nuclear matter with a compressibility around $215 MeV$ are reproduced.

A comparative study of the reactions $^{132}Sn + ^{132}Sn$ (EE system), $^{124}Sn + ^{124}Sn$ (HH) and $^{112}Sn + ^{112}Sn$ (LL) at $50 MeV/A$ is performed. The last two combinations were intensively analyzed in the recent years at MSU [17]. We shall focus at the value of impact parameter $b = 4 fm$ for which a typical behavior corresponding to the transition from multifragmentation to neck fragmentation, a process not very much investigated up to now, is clearly noted in our simulations. Indeed our previous results for these systems, indicate at $b = 4 fm$ a memory of entrance channel, through the existence of well defined PLF's and TLF's, even if the multiplicity of intermediate mass fragments is still quite large [23]. At $b = 6 fm$ the reaction mechanism corresponds to a neck fragmentation with mostly two or three IMF's observed in the mid-rapidity region and a short nucleus-nucleus interaction time.

Therefore, along this transition region, for impact parameters between $3 fm$ and $5 fm$, a mixing of features associated to multifragmentation and neck fragmentation are expected. The relative values of interaction time (of the order of $120 - 140 fm/c$), of the time associated to fragment formation and growth, as well as of the time scales for isospin migration and distillation, will determine the properties of emitted IMF's. Consequently, a good sensitivity to the symmetry energy density dependence can be expected.

III. FRAGMENTATION MECHANISM

A total number of 2000 events is generated for each entrance channel combination and equation of state at impact parameter $b = 4 fm$.

First, we adopt an analysis method of kinematic properties previously employed in studies concerning dynamical fission or neck fragmentation mechanisms [27, 28].

After the freeze-out time, corresponding to the saturation of the number of formed IMF's, we propagate the Coulomb trajectories of all fragments until a configuration where the Coulomb interaction becomes negligible. The asymptotic velocities of PLF and TLF define an intrinsic axis of the event by the vector $\mathbf{V}_{\mathbf{r}} = \mathbf{V}(H_1) - \mathbf{V}(H_2)$ always oriented from the second heaviest fragment H_2 toward the heaviest one H_1 . Even for mass symmetric entrance channels this is an appropriate defi-

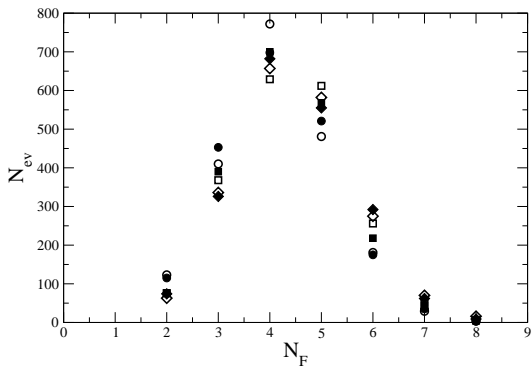


FIG. 1: Fragment multiplicity distribution at $b = 4fm$. Circles: $^{112}Sn + ^{112}Sn$. Squares: $^{124}Sn + ^{124}Sn$. Diamonds: $^{132}Sn + ^{132}Sn$. The filled symbols: asysoft EOS. The open symbols: asysuperstiff EOS.

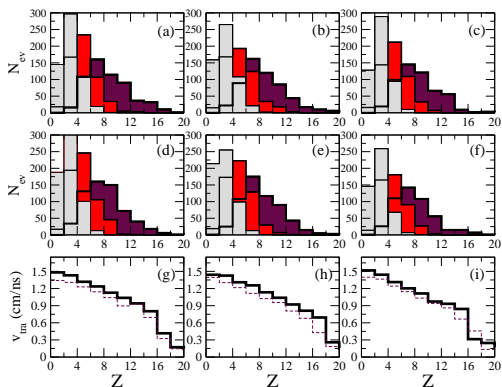


FIG. 2: The charge distribution for each IMF in hierarchy: asysoft EOS (upper row) and asysuperstiff EOS (middle row). HH combination: (a),(d),(g). EE combination: (b),(e),(h). LL combination: (c),(f),(i). Average transverse velocity distribution as a function of the charge (bottom row) for asysoft EOS (thick-solid line) and asysuperstiff EOS (thin-dashed line). All results refer to events with IMF multiplicity three. The histograms brighten as the rank of IMF's increases.

nition when searching for the correlations between kinematic properties of the IMF's and the break-up of the initial composite system. At freeze-out time the IMF's of each event are ordered in mass. The orthogonal and parallel components of their asymptotic velocities with respect to the intrinsic axis, v_{tra} and v_{par} , together with their charge Z , are determined. The events are classified according to the number of observed IMF's at freeze-out time. We report in Fig.1 the fragments multiplicity distributions associated to all studied cases. It is observed that more neutron rich systems favor larger IMF multiplicities. We select the classes with three IMF's (total number of fragments $N_F = 5$) and four IMF's ($N_F = 6$), corresponding to around 550 events and 250 events out of the total of 2000 events, providing so a reasonable statistics.

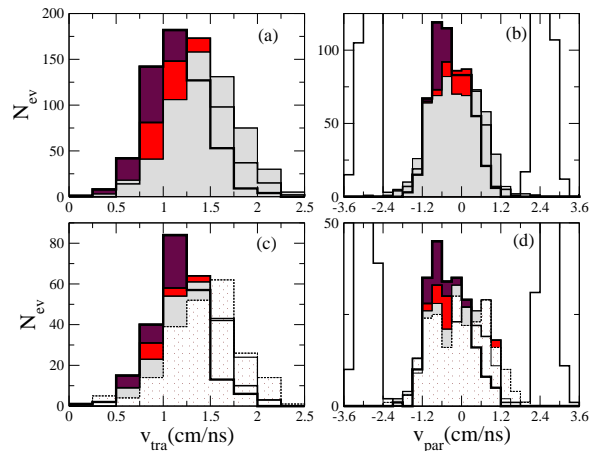


FIG. 3: HH combination and the asysoft EOS choice. Upper panels: fragmentation events with three IMF. (a) Transverse velocity v_{tra} distributions, (b) Parallel velocity v_{par} distributions. Bottom panels: events with four IMF. (c) v_{tra} distributions, (d) v_{par} distributions. The histograms brighten as the rank of IMF increases.

The charge distributions corresponding to each order in the mass hierarchy are shown in Fig.2, for the events with three IMF's and all entrance channel combinations, HH, EE and LL respectively. Let us mention that in the following, for all figures, the histograms brighten as the rank of IMF increases. The heaviest IMF (the rank one in hierarchy) can have a charge up to $Z = 16 - 18$ with distribution centered around $Z = 6 - 8$ while the lightest arrives up to $Z = 8$. In the bottom row of the figure is plotted the average transverse velocity in each charge bin calculated by considering all fragments independent of the position in hierarchy (see Fig.2 (g), (h) and (i)). The transverse velocity has a steep decreasing trend with the charge, in agreement with previous findings reported in [29], and does not depend much on the asy-EOS. In fact this appears to be one feature of the fragmentation dynamics. The larger transverse velocity of the lightest fragments seems to indicate a reduced driving effect of the PLF, TLF "spectators". All that can be related to the presence of a multifragmenting source located in the overlap region upon which the shape instabilities of the neck dynamics will take over. These observations require a more detailed investigation of the kinematic properties of fragments, once ordered in mass. As we shall see the correlations between velocity and size are amplified when analyzing the events according to the fragment rank in the hierarchy.

Figs.3 and 4 show, for asysoft and superasystiff EOS respectively, the IMF's transverse and parallel velocity distributions in the case of HH combination. We also report for reference, the parallel velocity distributions of projectile and target like residues as they result from our calculations at these energies.

For both classes of events considered, the transverse

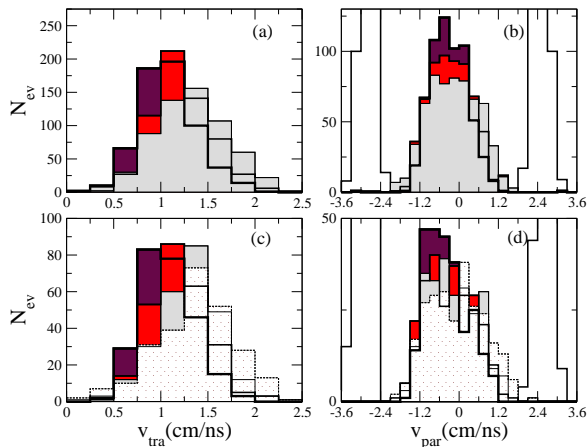


FIG. 4: Like Fig.3, for the asysuperstiff EOS choice.

velocity distribution shifts towards higher values with the IMF position in the mass hierarchy, the lightest fragment acquiring the greatest v_{tra} .

This hierarchy in the velocity perpendicular to the intrinsic axis emerges as a specific signal characterizing the transition from multifragmentation to neck fragmentation. It can be related to the peculiar geometrical configuration of the overlapping region and its fast evolution. The velocity distributions along the intrinsic axis are centered around the mid-velocity region, quite decoupled from the PLF and TLF. This is analogous to what is observed in neck fragmentation. The parallel velocity distribution of the lightest IMF looks broader and more symmetric around the center of mass velocity, suggesting a dominant volume contribution of spinodal and thermal nature to the fragment formation, like in multifragmentation. However, it is difficult to notice any hierarchy in the IMF velocity along the intrinsic axis.

The transverse velocity features were studied in more detail, by looking separately at in and out of reaction plane components, v_{tra} and v_{tray} , see Fig. 5. For both quantities we notice an interesting correlation to the fragment position in the hierarchy. This signal appears rather robust, since in order to increase the statistics we integrate over the whole v_{par} distribution of Fig. 3. For light fragments, the distribution of transverse velocity in reaction plane appears much more extended than that associated to the component orthogonal to the reaction plane. Just the opposite behavior is observed for the heavier fragments of the hierarchy. The presence of the larger transverse velocities on the reaction plane for the lightest masses in the hierarchy seems to point towards an incomplete dissipation of the entrance channel collective energy flux. This would be consistent with the formation of light fragments via a faster multifragmentation mechanism. Conversely, larger out of reaction plane velocities for the heaviest masses reflect their formation on longer time scales, with more initial collective energy dissipated and larger Coulomb effects. In spite of this,

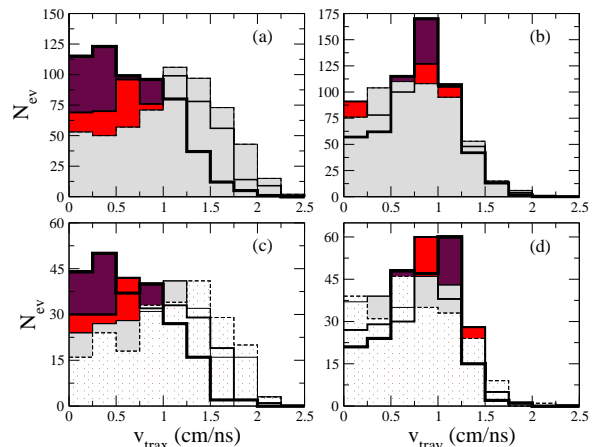


FIG. 5: The asysoft EOS and HH combination. Transverse velocity in reaction plane distribution for fragmentation events with three IMF (a) and four IMF respectively (c). Transverse velocity out of reaction plane distribution for fragmentation events with three IMF (b) and four IMF (d).

when the two components are combined to generate the final distributions in transverse velocity, the hierarchy signal is rather robust, see Figs. 3,4. This suggests that the rate at which the fragments depart from the intrinsic axis is essential and this depends on their rank in mass hierarchy.

To gain more insight into the competition between thermal and dynamical, non-equilibrium effects, we analyzed the collective flow properties associated to the IMF's. For each rank in mass hierarchy the transverse and elliptic flows parameters were obtained as:

$$v_1 = \langle \frac{p_x}{p_T} \rangle; \quad v_2 = \langle \frac{p_x^2 - p_y^2}{p_T^2} \rangle, \quad (3)$$

where p_x now refers to the in-reaction plane component of the momentum perpendicular to the beam axis, while p_y is momentum component orthogonal to the reaction plane. Here $p_T = \sqrt{p_x^2 + p_y^2}$ is the transverse momentum and the average was performed over the number of events. The different behavior of the IMF's transverse velocity components, for various positions in the mass hierarchy discussed above should be clearly distinguished in the flows.

In Fig.6 we report the in plane transverse flow v_1 as a function of the fragment velocity along beam axis v_z , for each rank in mass hierarchy with three IMF's. The light fragments present an almost flat, close to zero transverse flow, fully consistent with an early formation and decoupling in the mid-rapidity zone. At variance, the heavy fragments nicely follow positive/negative value due to the correlation to the PLF/TLF spectators. In Fig.7 we represent the elliptic flow parameter v_2 dependence on the total transverse velocity $v_T = \sqrt{v_x^2 + v_y^2}$, again for each of the three orders in hierarchy. For small v_T

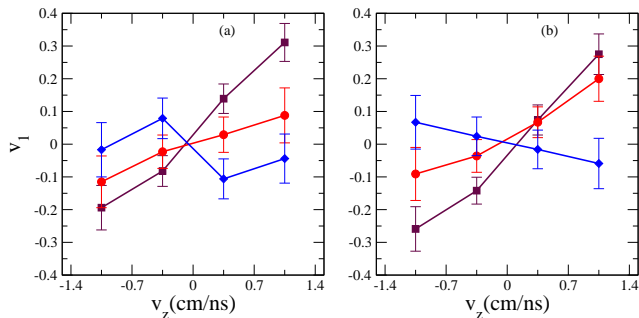


FIG. 6: Direct flow parameter v_1 as a function of velocity along beam axis v_z . HH combination and events with three IMF's. Squares: heaviest IMF. Circles: second heaviest IMF. Diamonds: the lightest IMF in hierarchy. (a) Asysoft EOS, (b) Asysuperstiff EOS. See the text.

the elliptic flow is negative, indicating a behavior dominated by the thermal expansion out of reaction plane. However, the value of the anisotropy parameter v_2 increases with the position in hierarchy in a given bin of v_T . It also rises with the transverse velocity, becoming positive above $v_T \approx 1.4 \text{ cm/ns}$. This feature can be related to the incomplete dissipation of entrance channel collective energy, driving lighter fragments easier parallel to the reaction plane. We have to look at this figure also in connection to Fig. 2 (bottom panel) where the v_{tra} distribution versus charge is presented. Light fragments, more abundant at high transverse velocities clearly show positive elliptic flow fully consistent with the analysis of Fig. 5. Heavier fragments, more abundant at lower v_{tra} nicely show more negative v_2 values, again in agreement with the results of Fig. 5. All these features should be considered as specific to this fragmentation mechanism. We stress that it is likely to exist some other production mechanisms, with properties differing from those evidenced above, but not described by our transport model. These include breakup or fission of strongly deformed quasiprojectile/quasitargets, which take place on longer time scales as well as statistical decay of the primary fragments. However it is hoped that a proper selection of kinematic characteristics can single out various classes of events.

IV. ISOSPIN EFFECTS

As already noted, the features discussed above are determined mainly by the isoscalar part of the equation of state. On top of that the symmetry energy induces various changes on the properties related to the isospin content of the fragments. We have extended our investigations to isospin observables studying their dependence on the IMF position in hierarchy as well the correlation to transverse velocity. In Figs. 8, (for asysoft EOS) and 9 (for asysuperstiff EOS) we report the asymmetry

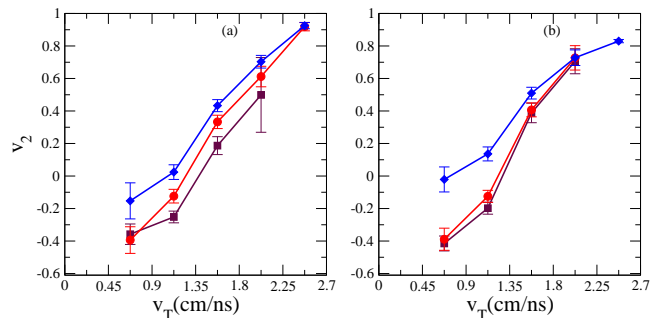


FIG. 7: HH combination and events with three IMF's: elliptic flow anisotropy parameter v_2 as a function of transverse velocity v_T . Squares: heaviest IMF. Circles: second heaviest IMF. Diamonds: the lightest IMF in hierarchy. (a) Asysoft EOS. (b) Asysuperstiff EOS.

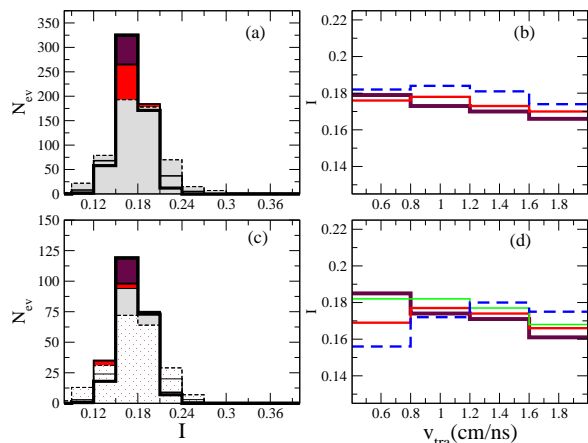


FIG. 8: HH combination in the asysoft EOS choice. Upper panels: events with three IMF. (a) Isospin distribution. (b) Fragment isospin content as a function of transverse velocity. Bottom panels: events with four IMF. (c) Isospin distributions; (d) Fragment isospin content vs transverse velocity. All histograms are like in the caption of Fig. 3. The dashed lines correspond to the lightest IMF. A thinner continuous line is associated with a lighter IMF.

$I = (N - Z)/(N + Z)$ distribution of each IMF of the hierarchy. The results refers again to HH system whose initial asymmetry is $I = 0.194$. Several differences between the two asy-EOS are evidenced. For asysoft EOS the isospin distributions are centered at a lower value and their widths are rather narrow. At variance, for asysuperstiff EOS the centroids of the distributions are closer to the initial value of the composite system and their broader widths depend on the position in the mass hierarchy. For both asy-EOS the lightest IMF's are more likely to acquire higher values of the asymmetry. We also notice that similar results were obtained for the other entrance channel combinations, LL and EE respectively.

We relate these features to the differences between the two asy-EOS at sub-saturation densities. Clearly,

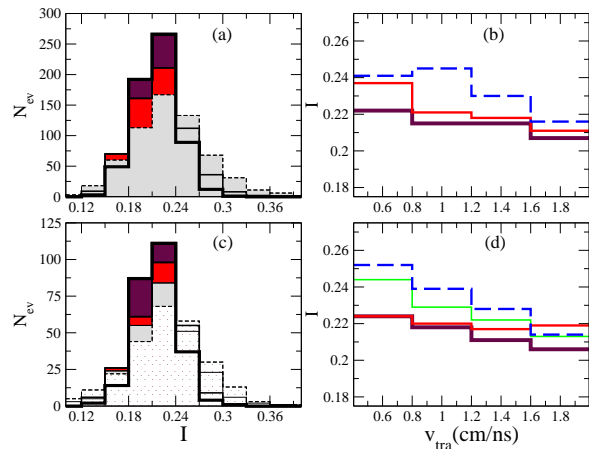


FIG. 9: Like in Fig.8, for the asysuperstiff EOS choice.

a larger value of the symmetry energy will fasten the isospin distillation process and all IMF's reach lower and closer values of the asymmetry. This is the case for the asysoft EOS. On the other hand larger values of fragment asymmetry in the case of asysuperstiff EOS shows that this was not very effective during the formation phase.

The fragments continue to grow in quite low density, more asymmetric regions, as a result of isospin migration. The differences inside the hierarchy for the latter asy-EOS point towards different formation time scales, with the lightest IMF finding more neutron rich environment and a distillation process not fast enough to produce the same asymmetry for all IMF's in the event. However, it is interesting to remark that these fragments also acquire the largest transverse velocity, as it was discussed before. Therefore a possible scenario is that they escape faster from the active region keeping a partial memory of the early conditions of the fragmentation. At variance, if they have lower transverse velocity and appearing in a richer neutron region, will carry higher asymmetry. We represent the average asymmetry as a function of transverse velocity in Figs. 8 and 9, for asysoft and asysuperstiff EOS choice respectively.

A decreasing trend is generally observed for the IMF's, more pronounced for asysuperstiff EOS. Moreover, in this case, the trend is particularly evident for the lightest IMF's, in agreement with the previous discussion.

For a given transverse velocity bin the asymmetry always increases with the rank in hierarchy in the case of asysuperstiff EOS. On the other hand, for the asysoft EOS we cannot appreciate much such differences, all fragments reaching almost the same asymmetry.

The same type of analysis has been carried out for the LL combination aiming to construct isotopic double ratios and to study their dependence on the transverse velocities. Concerning the fragment isotopic content, similar differences between the two asy-EOS, as observed for the HH combination, were evidenced, in spite of the fact that Coulomb effects are now more important. We also

observed an analogous trend of the fragment asymmetry with the transverse velocity. Therefore, in this case the double ratios do not show appreciable differences between the two asy-EOS. The same conclusion was reached in central collisions [20]. However, as we noticed before, differences can be evidenced even within the same system, by comparisons between fragments belonging to different ranks in hierarchy for various kinematic selections.

V. CONCLUSIONS AND PERSPECTIVES

In this paper, by employing a microscopic transport model, we unveiled new features of nuclear fragmentation in semi-central to semi-peripheral collisions from the study of several kinematic correlations of intermediate mass fragments.

At Fermi energies, an almost continuous transition with the centrality, from multifragmentation to neck fragmentation mechanisms, is revealed. Good observable tracers appear to be related to the correlations between the fragment masses, transverse velocities and isospin contents. In fact, specific hierarchy phenomena are signaled: the distributions of the velocity perpendicular to the intrinsic axis of the event depend on the rank in a mass hierarchy of the event. In the reaction plane the lightest fragments acquire greater transverse velocities, a phenomenon observed for several mass entrance channels. This feature can be used as an identification of the fragmentation mechanism discussed in this paper.

Another important finding is that the fragment isospin content is sensitive to the position in this hierarchy and this can be related to the density dependence of symmetry energy at sub-saturation densities as well as to the relative time scales for fragment formation and isospin transport.

These observations open new opportunities from the experimental point of view. An analysis of isospin dependent observables in correlation to position in mass hierarchy or kinematic observables may add other constraints upon the behavior of symmetry energy below normal density and can provide a supplementary support for the assumption that the IMF's form in the low density regions of heated nuclear matter. We mention that recent experimental results, reported by CHIMERA collaboration for the system $Sn + Ni$ at a lower energy (35 AMeV) [30], sustain the existence of the hierarchy in transverse velocity, as discussed in this paper. Their analysis also signaled differences in the isospin content of IMF's when ordered in a mass hierarchy, the lightest fragments being more asymmetric. This kind of observations support an asystiff-like behavior of the symmetry energy at sub-saturation densities.

Acknowledgments

The authors are grateful to E. De Filippo, A. Pagano, P. Russotto, and CHIMERA Collaboration for stimulating discussions. One of authors, V. Baran thanks for warm hospitality at Laboratori Nazionali del Sud. This work was supported in part by the Romanian Ministry for Education and Research under the CNCSIS contract

PN II ID-1038/2008. For R. Zus this work was supported by the strategic grant POSDRU/89/1.5/S/58852, Project "Postdoctoral programme for training scientific researchers" co-financed by the European Social Found within the Sectorial Operational Program Human resources Development 2007-2013.

-
- [1] V. Baran, M. Colonna, M. Di Toro, V. Greco, Phys. Rep. **410** 335 (2005).
- [2] A.W. Steiner, M. Prakash, J.M. Lattimer, P.J. Ellis Phys. Rep. **411** 325 (2005).
- [3] Bao-An Li, Lie-Wen Chen, Che-Ming Ko, Phys. Rep. **464** (2008) 113.
- [4] P. Chomaz, M. Colonna, J. Randrup, Phys. Rep. **389** 263 (2004).
- [5] A.H. Raduta, M. Colonna, M. Di Toro, Phys. Rev. C **76** 024602 (2007).
- [6] J. Frankland et al., Nucl. Phys. A **689** 940 (2001); B. Borderie et al., Phys. Rev. Lett. **86** 3252 (2001).
- [7] V. Baran, M. Colonna, M. Di Toro, A.B. Larionov, Nucl. Phys. A **632** 287 (1998).
- [8] V. Baran, M. Colonna, M. Di Toro, V. Greco, Phys. Rev. Lett. **86** 4492 (2001).
- [9] E. De Filippo et al., Phys. Rev. C **71** 044602 (2005).
- [10] M. Di Toro, A. Olmi, R. Roy, Eur. Phys. J. A **30** 65 (2006).
- [11] P. Milazzo et al., Nucl. Phys. A **703** 466 (2002).
- [12] P. Russotto et al. (Chimera Coll.), Phys. Rev. C **81** 064606 (2010).
- [13] V. Baran, M. Colonna, M. Di Toro, Nucl. Phys. A **730** 329 (2004).
- [14] M. Papa et al., Phys. Rev. C **75** 054616 (2007).
- [15] E. De Filippo et al., Phys. Rev. C **71** 064604 (2005).
- [16] P. Russotto et al. (Chimera Coll.), Int. J. Mod. Phys. E **15** 410 (2006).
- [17] M.B. Tsang et al., Phys. Rev. Lett. **92** 062701 (2004); M.B. Tsang et al., Phys. Rev. Lett. **102** 122701 (2009).
- [18] V. Baran et al., Phys. Rev. C **72** 064620 (2005).
- [19] J. Rizzo et al, Nucl. Phys. A **806** 79 (2008).
- [20] M. Colonna et al., Phys. Rev. C **78** 064618 (2008).
- [21] J. Colin et al. (INDRA Coll.), Phys. Rev. C **67** 064603 (2003).
- [22] A.B McIntosh et al., Phys. Rev. C **81** 034603 (2010).
- [23] V. Baran et al., Nucl. Phys. A **703** 603 (2002).
- [24] J. Rizzo, Ph. Chomaz, M. Colonna, Nucl. Phys. A **806** 40 (2008) and refs. therein.
- [25] M. Colonna et al., Nucl. Phys. A **642** 449 (1998).
- [26] M. Colonna, M. Di Toro, G. Fabbri, S. Maccarone, Phys. Rev. C **57** 1410 (1998).
- [27] A.A. Stefanini et al. Z. Phys. A **351** 167 (1995).
- [28] J. Wilczynski et al, (CHIMERA Coll.) Int. J. Mod. Phys. E **14** 353 (2005).
- [29] R. Lioni et al., Phys. Lett. B **625** 33 (2005).
- [30] E. De Filippo et al. (CHIMERA Coll.), Invited talk at IWM 2009, Catania, Italy. SIF Conf. Proceedings vol. 101, Bologna 2010, pg. 178-188. E. De Filippo, P. Russotto, private communication .